

Charge Ordering and Spin Dynamics in NaV_2O_5

B. Grenier^a, O. Cepas^b, L.P. Regnault^a, J.E. Lorenzo^c, T. Ziman^b, J.P. Boucher^d, A. Hiess^b, T. Chatterji^b, J. Jegoudez^e and A. Revcolevschi^e

^aDépartement de Recherche Fondamentale sur la Matière Condensée, SPSMS, Laboratoire de Magnétisme et de Diffraction Neutronique, CEA-Grenoble, F-38054 Grenoble cedex 9, France.

^bInstitut Laue Langevin, BP 156, F-38042 Grenoble cedex 9, France.

^cLaboratoire de Cristallographie, CNRS, BP 166, F-38042 Grenoble cedex 9, France.

^dLaboratoire de Spectrométrie Physique, Université J. Fourier Grenoble I, BP 87, F-38402 Saint Martin d'Hères cedex, France.

^eLaboratoire de Physico-Chimie de l'Etat Solide, Université Paris-Sud, Bât 414, F-91405 Orsay cedex, France
(June 2000)

We report high-resolution neutron inelastic scattering experiments on the spin excitations of NaV_2O_5 . Below T_c , two branches associated with distinct energy gaps are identified. From the dispersion and intensity of the spin excitation modes, we establish that the charge order characterizing this low- T phase corresponds to a *zig-zag* distribution on the ladder rungs. It is also shown that the spin gaps are primarily determined by the charge transfer, which is evaluated to be important.

PACS numbers: 71.45.Lr, 75.10.Jm, 75.40.Gb

The low dimensional inorganic compound NaV_2O_5 undergoes a phase transition at $T_c = 34$ K [1] associated with both a lattice distortion [2] and the opening of an energy gap to the lowest triplet spin excitations [3]. While the nature of the low- T phase in NaV_2O_5 is not fully understood it is clear that, unlike CuGeO_3 [4], the spin-Peierls model does not apply simply to this compound [5]. Mostovoy and Khomskii [6] suggested that the spin gap could result from charge-order (CO) rather than the lattice distortion. Indeed, NMR measurements indicate two inequivalent vanadium sites below T_c , while there exists only one site above [7]. There has been no direct evidence for the connection between CO and a spin gap, nor to distinguish various conjectured spatial distributions of charge [8,6]. In this letter, we present new results of neutron inelastic scattering (NIS) on the spin excitations in the low- T phase that can now resolve these issues. Since the dynamics of charge and spin are well separated in frequency, the intensities of the spin excitations can determine the form and magnitude of static charge order and test quantitatively theories of the spin gap. From the dispersion, we can estimate the couplings parallel and transverse to the strongly coupled direction.

In NaV_2O_5 , the vanadium ions have a formal valence of 4.5+. Initially, this was proposed to correspond to an alternation of V^{4+} ions, with a spin value $S = 1/2$, and V^{5+} ions with $S = 0$ [9]. At room temperature, NaV_2O_5 is well described by a quarter-filled two-leg ladder system, with only one type of vanadium site $\text{V}^{4.5+}$ [10]. From calculations of electronic structure [11], the strongest orbital overlaps are on the ladder rungs. One expects that the $S = 1/2$ spins are carried by the V-O-V molecular bonding orbitals, with charge fully delocalized on two sites. As the energy of the anti-bonding orbital is much higher, it can be projected out, and above T_c , these spins, as they interact in the leg direction ($\parallel \mathbf{b}$ axis), form

an effective uniform quantum Heisenberg spin *chain* [12] with interactions between chains that are both weaker and frustrated.

At low temperatures, NMR shows this can no longer be so. On each rung, a charge disproportionation Δ_c may occur, defined through $n_{\pm} = (1 \pm \Delta_c)/2$, where n_{\pm} are the average charges on each vanadium site. Two forms of CO can be considered, the *in-line* [8], with the same charge transfer on each rung, and the *zig-zag* [6] with alternation in the charge along the ladders as shown in fig. 1b. Recent X-ray diffraction measurements [13] established that the lattice structure below T_c consists of a succession of distorted and non-distorted ladders of vanadium ions (see fig. 1a). Neglecting inter-ladder diagonal couplings J_{\perp} , the ladders would behave magnetically as independent spin chains. For one ladder (chain 2 in fig. 1a) distortions in the exchange paths both within the ladder and via neighboring ladders result in an alternation of the effective exchange coupling in the \mathbf{b} direction, J_{b1} and J_{b2} . The ladders in which the rungs are distorted (chains 1 and 3), however, remain magnetically uniform as a mirror plane passes through each rung. A *minimum* magnetic model without CO would be a succession of alternating and uniform chains. An energy gap (expected to be small as it results primarily from the alternation in J_{\perp}) would characterize the excitation branch of the alternating chains, and there would be no gap for the uniform chains. The initial NIS [3] found, however, two excitation branches, with the same gap at the antiferromagnetic point $E_g^+ = E_g^- \approx 10$ meV. To analyze these results, a recent spin model [14] used an explicit relation between the spin excitations and the CO. This model assumed a single gap and is ruled out by the NIS data as it implies zero intensity of one excitation branch. A more precise determination of excitations in the low- T phase of NaV_2O_5 is therefore crucial. In the present

work, using high-resolution conditions, the dispersion of the excitations is re-explored in a wider part of the reciprocal space. Moreover, the structure factor, i.e., the (energy-integrated) intensity of each excitation mode, is evaluated. The disproportionation factor Δ_c can then be directly determined.

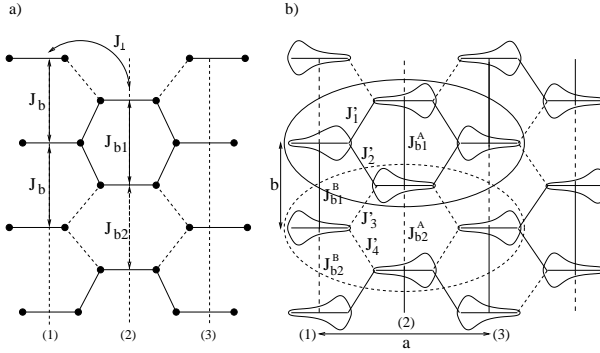


FIG. 1. a) Simplified representation of distorted and non-distorted chains, chain 1 (or 3) and 2, respectively, with the J_{\perp} bond alternation between chains 1 and 2; b) Proposed charge order (large and small lobes represent large and small average charges) leading to a spin gap. The elementary translation (a,b) of this CO agrees with the observed periodicity of spin excitations.

The single crystal used in this study ($\approx 8 \times 5 \times 2 \text{ mm}^3$) was grown by a flux method. The NIS measurements were performed on two thermal neutron three-axes spectrometers - IN8 and CRG/CEA-IN22 - both installed at the Institut Laue-Langevin (ILL). On IN8, vertically focusing monochromator PG(002) and Cu(111) were used in conjunction with a vertically focusing analyzer PG(002) and horizontal collimations $60'-40'-60'$. The final wave vector was kept fixed at $k_f = 4.1 \text{ \AA}^{-1}$. IN22 was operated at $k_f = 2.662 \text{ \AA}^{-1}$, with a PG(002) analyzer used in horizontal monochromatic focusing condition with no collimation. The sample was installed in an “orange” ILL cryostat, with the scattering wave-vector \mathbf{Q} lying in the reciprocal (a^*, b^*) ladder plane.

The two branches characterizing the low-energy excitations in NaV_2O_5 have distinct energy gaps: $E_g^+ \neq E_g^-$. This important result will be established when we consider the dispersions in the transverse \mathbf{a} direction. First, however, we determine the dispersion in the leg direction (\mathbf{b} axis). Examples of constant-energy scans obtained on IN8 as a function of Q_b are displayed in fig. 2a (wave-vector components are expressed in reciprocal lattice units, r.l.u.). Increasing the energy, one resolves the single peak seen at 10 meV into propagating modes (dashed lines), whose peak position is shown in fig. 2b. They describe the dispersion of the elementary excitations in the \mathbf{b} direction, near the AF chain wave-vector component Q_b^{AF} ($\equiv Q_b = 0.5$). They are compared to a dispersion law characteristic of a gapped spin chain:

$E(q_b) = \sqrt{E_g^2 + (E_m^2 - E_g^2) \sin^2(2\pi Q_b)}$ where E_g and E_m are the gap and maximum energies of the dispersion, respectively. For both $E_g = E_g^+$, E_g^- (the solid and dashed lines, respectively), we evaluate $E_m = 93 \pm 6$ meV. Compared to the prediction for an uniform Heisenberg chain, $E_m = \pi J_b/2$, where J_b is the exchange in the chain, one obtains for the low- T phase, $J_b \approx 60$ meV.

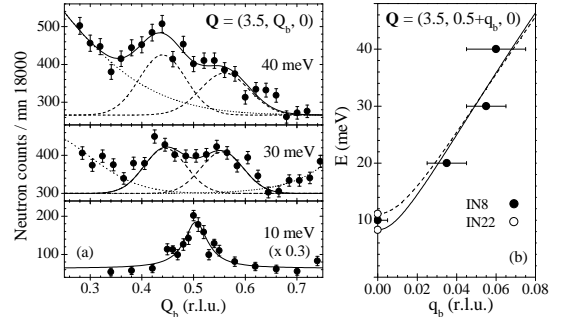


FIG. 2. a) Constant-energy scans as a function of Q_b . The dotted lines represent the background. The other curves are fit to the data; b) Energy dispersion in the \mathbf{b} direction. The lines correspond to the two branches with gaps E_g^+ and E_g^- .

Second, we consider the dispersions in the \mathbf{a}^* direction (i.e., along the rungs). A few examples of energy scans performed on IN22 at constant \mathbf{Q} are reported in fig. 3. In general, two peaks are observed. At a few Q_a values, however, an extinction occurs. This extinction may concern one of the two modes, or the two modes simultaneously. The left and right panels report data obtained for $Q_b^{AF} = 0.5$ and $Q_b = 1$ (equivalent to the zone center of the AF chains Q_b^{ZC}). As examples, we show for Q_b^{AF} that the smallest energy difference between the two observed peaks is obtained for *integer* Q_a values (here, $Q_a = 3$), the largest one for *half-integer* values ($Q_a = 2.5$) and an extinction of the two modes occurs at $Q_a \approx 1.75$ (identical results have been obtained for $Q_b = 1.5$). Surprisingly, at the chain zone-center Q_b^{ZC} we found a small but non-zero intensity for the two excitation branches. The smallest energy difference between the two peaks is now obtained for *half-integer* values (here, $Q_a = 1.5$). Extinctions of one of the two modes is observed at $Q_a = 1$ (on the high-energy mode) and at $Q_a = 2$ (on the low-energy mode). For all the recorded spectra, the background shown as the dotted lines was carefully determined.

For the analysis, we assume the two observed peaks to belong to two distinct contributions. Their unsymmetrical lineshape is characteristic of gapped excitations undergoing a rapid energy dispersion (as established in fig. 2b). In such a case, a dynamical response function (shown by the dashed lines in fig. 3) is well-suited to fitting, conveniently defined with only 3 parameters: the peak energy E_+ (E_-), an intensity factor A_+ (A_-) and an energy damping Γ . As Γ is mainly fixed by the

resolution conditions, it is assumed to be the same for the two contributions ($\Gamma \approx 0.4 - 0.8$ meV). Together with the background, the agreement with the experiments, shown by the solid lines, is good. The values obtained for E_{\pm} as a function of Q_a are shown in fig. 4. We establish several new features. At both Q_b^{AF} (solid symbols) and Q_b^{ZC} (open symbols), the transverse dispersion consists of two distinct excitation branches which never cross. This justifies our previous statement, namely that there are *two* distinct energy gaps, E_g^+ and E_g^- . In each branch, the periodicity is $2\pi Q_a$: this is twice that previously determined. The two dispersions have the same amplitude, $\delta J \approx 1$ meV but, remarkably, the upper and lower branches are out of phase, and there is phase inversion between branches at Q_b^{ZC} and Q_b^{AF} . For each excitation branch, the corresponding structure factors, $S_{b\pm}^{AF}(Q_a)$ and $S_{b\pm}^{ZC}(Q_a)$ are evaluated by integrating the fitted dynamical response functions over a wide energy range (from 0 up to $E \approx 300\Gamma$). The resulting values (dots and squares) are reported in figs. 5a and b. The sums $S_b^{AF}(Q_a) = S_{b+}^{AF}(Q_a) + S_{b-}^{AF}(Q_a)$ and $S_b^{ZC}(Q_a) = S_{b+}^{ZC}(Q_a) + S_{b-}^{ZC}(Q_a)$ are shown as the stars.

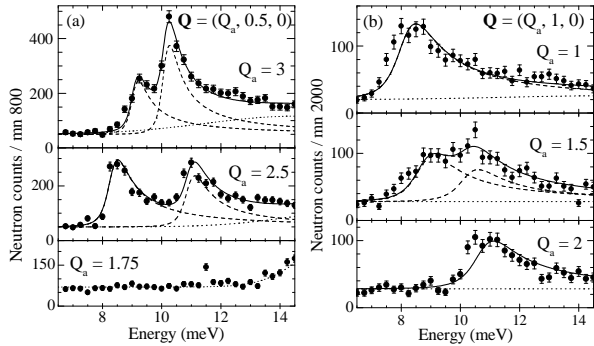


FIG. 3. Constant- \mathbf{Q} scans as function of energy: a) at $Q_b \equiv Q_b^{AF}$; b) at $Q_b \equiv Q_b^{ZC}$. Curves are described in text.

The interpretation of these results is developed in three steps. First, the charge order: each spin is associated with an electronic wave function on the two sites of a rung that depends on n_{\pm} . The structure factors for the *in-line* and *zig-zag* models are $S_{Q_b}(Q_a, \omega) = \cos^2(\pi Q_a \rho) \tilde{S}(Q_a, Q_b, \omega) + \Delta_c^2 \sin^2(\pi Q_a \rho) \tilde{S}(Q_a + \frac{1}{2}, Q_b, \omega)$ and $S_{Q_b}(Q_a, \omega) = \cos^2(\pi Q_a \rho) \tilde{S}(Q_a, Q_b, \omega) + \Delta_c^2 \sin^2(\pi Q_a \rho) \tilde{S}(Q_a + \frac{1}{2}, Q_b + \frac{1}{2}, \omega)$, respectively, where $\rho = l/a \approx 0.304$ (l , rung length and a , lattice parameter) and $\tilde{S}(Q_a, Q_b, \omega)$ is the structure factor for spins localized on the center of each rung. From the ratios of intensities for different values of momentum, one can extract the charge transfer Δ_c independent of the form of \tilde{S} . In particular, we verify that the order cannot be *in-line* but predictions agree with a *zig-zag* order with $\Delta_c^2 \approx 0.35$, i.e., $\Delta_c \approx 0.6$. The agreement is particularly good for the sums $S_b^{AF}(Q_a)$ and $S_b^{ZC}(Q_a)$.

For the absolute intensities, we need an explicit form for \tilde{S} which we take from the strongly dimerized limit (SDL), in which the wave function is simply a product of singlets on the stronger bonds. For the *in-line* model, for example, the SDL would give zero intensity at Q_b^{ZC} in contradiction with the observation (the data in fig. 5b). The *in-line* model can be ruled out. In figs. 5a and b, the predictions provided by the *zig-zag* model (solid lines) are compared with the experimental total structure factors $S_b^{AF}(Q_a)$ and $S_b^{ZC}(Q_a)$ (solid and open stars). In fig. 5a, the agreement is obtained with no adjustable parameter except for an overall amplitude factor. Once this factor is determined, the results in fig. 5b depends only on Δ_c^2 . As can be seen, a good agreement is obtained for $\Delta_c^2 \approx 0.35$. The low-T phase of NaV_2O_5 is very well described by the *zig-zag* model, with a rather large charge transfer.

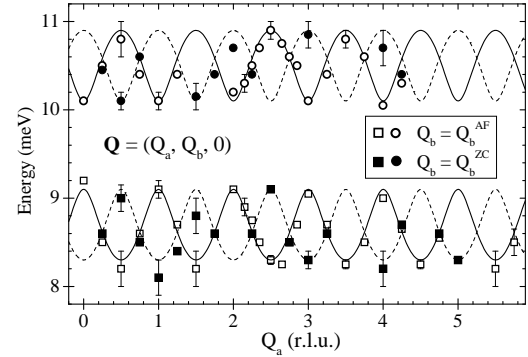


FIG. 4. Dispersion of the two excitation branches in the a direction at Q_b^{AF} and Q_b^{ZC} . The curves are theoretical predictions fitted to the data (see text).

Second, we consider the transverse dispersions. Later, we explain that the gap is induced by the CO. In fact, there are two distinct gaps because of the structural distortions (implying distinct couplings $J_{b1,2}^A$ and $J_{b1,2}^B$ as shown in fig. 1b). Due to the CO (see fig. 1a), 4 different interchain exchange integrals must be considered, J'_1 , J'_2 , J'_3 and J'_4 . The two branches (associated with the gaps E_g^+ and E_g^-) acquire a transverse dispersion, described at Q_b^{AF} and Q_b^{ZC} by $E_{b\pm}^{AF} = (E_g^+ + E_g^-)/2 \pm \sqrt{(E_g^+ - E_g^-)^2/4 + \delta J^2 \sin^2(\pi Q_a/2)}$ and $E_{b\pm}^{ZC} = (E_g^+ + E_g^-)/2 \pm \sqrt{(E_g^+ - E_g^-)^2/4 + \delta J^2 \cos^2(\pi Q_a/2)}$, respectively, with $\delta J = J'_1 - J'_2 + J'_3 - J'_4$. In fig. 4, these predictions (solid and dashed lines) are compared to the data. Again, a very good agreement is obtained yielding the following evaluation $E_g^+ = 10.1 \pm 0.1$, $E_g^- = 9.1 \pm 0.1$ and $\delta J = 1.2 \pm 0.1$ meV. The dispersion gives directly the *alternation* in the inter-ladder diagonal bonds δJ . If we assume it is dominated by the CO, we can also estimate the *average* from $\delta J \approx J_{\perp} \Delta_c^2$ [14] giving $J_{\perp} \approx 2.4$ meV.

The structure factors can be calculated for each branch. Within the SDL approach, one obtains the con-

tributions $S_{b\pm}^{AF}(Q_a)$ and $S_{b\pm}^{ZC}(Q_a)$ [15] shown by the dotted and dashed lines in fig. 5. In fig. 5b, the agreement with the data is rather good. In particular, the extinction phenomenon observed for each branch is well reproduced. In fig. 5a, we note a discrepancy between the SDL predictions and the individual structure factors $S_{b+}^{AF}(Q_a)$ and $S_{b-}^{AF}(Q_a)$ while the sum $S_b^{AF}(Q_a)$ is well described.

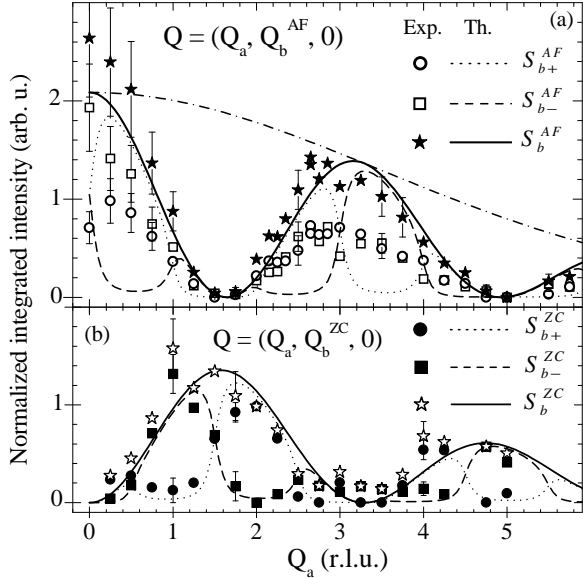


FIG. 5. Structure factors $S_{b\pm}^{AF}(Q_a)$ and $S_{b\pm}^{ZC}(Q_a)$ for the two magnetic branches in the **a** direction: a) at Q_b^{AF} ; b) at Q_b^{ZC} . The solid and open stars represent the sums $S_b^{AF}(Q_a)$ and $S_b^{ZC}(Q_a)$. The data are corrected from the V^{4+} atomic form factor $f_{V^{4+}}$, being all normalized at $Q_b = 0.5$. The dot-dashed line gives the Q_a dependence of $f_{V^{4+}}$. The other curves are theoretical predictions compared to the experiments (see text).

Finally, we consider the origin of the gap. As discussed in the introduction, the lattice distortion alone, in isolated ladders, cannot explain the presence of two energy gaps and their size. To analyze the effects of the diagonal couplings J_\perp , we refer to fig. 1b. Each ladder is seen to be a succession of two distinct clusters (shown by ovals in the figure). By exact diagonalization of each cluster, using the effective parameters of a t-J model, calculated from the high temperature structure [11] and adding a potential imposing a charge transfer, we evaluated J_{b1} and J_{b2} as a function of Δ_c . The bond alternation is defined as $d = |J_{b1} - J_{b2}| / (J_{b1} + J_{b2})$. For $\Delta_c \approx 0.6$, $d \approx 0.025 - 0.030$. The couplings underestimate the experimental value $J_b \approx 60$ meV measured here by a factor of about 2, but as the parameters are based on high temperature geometries and are, in any case, limited in accuracy, the agreement is satisfactory. The bond alternation can be considered as providing a reasonable estimate. Using the experimental value of J_b and the calculated

alternation $d \approx 0.025 - 0.030$ one finds an energy gap $E_g \approx 6 - 8$ meV. This is in a fairly good agreement with the experimental value $E_g \approx 10$ meV. This simple analysis shows that, in NaV_2O_5 , the gaps are primarily due to the CO. The lattice distortion plays here a secondary role, explaining why two distinct branches are observed experimentally, and their separation. As shown in fig. 1b, two successive chains are not identical. This should result in slightly different Δ_c . It is possible that the difficulty noted in reproducing individual intensities in fig. 5a are related to differing Δ_c . In our analysis, however, we have excluded such differences on the basis of NMR results which show only two charges [7] on the three crystallographic inequivalent sites [13]. Finally, note that the proposed CO spontaneously lowers the crystal symmetry defined by atomic positions. It would be interesting to verify this by other means, e.g. X-ray diffraction.

In conclusion, we have shown that the CO can be determined quantitatively by NIS. In the low-T phase of NaV_2O_5 , it corresponds to the zig-zag model sketched in fig. 1a, with $\Delta_c \approx 0.6$ and this order explains the energy gaps. The three scales of the low energy excitations: the average of the two gaps, their separation and the dispersion in the weakly coupled direction are directly related to the charge order, the lattice distortion and the alternation in the diagonal couplings J_\perp , respectively.

- [1] M. Isobe and Y. Ueda, J. Phys. Soc. Jpn **65**, 1178 (1996).
- [2] T. Chatterji et al., Solid State Com. **108**, 23 (1998).
- [3] T. Yosihama et al., J. Phys. Soc. Jpn **67**, 744 (1998).
- [4] For a review, see J.P. Boucher and L.P. Regnault, J. Phys. I France **6**, 1939 (1996).
- [5] S.G. Bompard et al., unpublished, cond-mat/9911298.
- [6] Mostovoy and Khomski, cond-mat/9806215 (unpublished); Damascelli et al. Phys. Rev. Lett. **81**, 918 (1998).
- [7] T. Ohama et al., Phys. Rev. B **59**, 3299 (1999).
- [8] P. Thalmeier and P. Fulde, Europhys. Lett., **44**, 142 (1998); H. Seo and K. Fukuyama, J. Phys. Soc. Jpn **67**, 2602 (1998).
- [9] P.A. Carpy and J. Galy, Acta Crystallogr B **31**, 1481 (1975).
- [10] H. Smolinski et al., Phys. Rev. Lett. **80**, 5164 (1998).
- [11] N. Suaud and M.B. Lepetit, Phys. Rev. in press (2000).
- [12] D.C. Johnston et al., unpublished, cond-mat/0003271.
- [13] J. Lüdecke et al., Phys. Rev. Lett. **82**, 3633 (1999).
- [14] C. Gros and R. Valenti, Phys. Rev. Lett. **82**, 976 (1999).
- [15] The corresponding expressions agrees with the sum rules $S_b^{AF}(Q_a)$ and $S_b^{ZC}(Q_a)$ established above.
- [16] In T. Ohama et al., cond-mat/0003141, the CO proposed in model Z2 (fig. 3) does not give rise to energy gaps, model Z3 provides a gap for only one out of two chains, model Z1 is the same as our.